A Low-Cost Potentiostat for Point-of-Need Diagnostics

P. Bezuidenhout, S. Smith, K. Land
Materials Science and Manufacturing,
Council for Scientific and Industrial Research (CSIR),
Pretoria, South Africa
pbezuidenhout@csir.co.za

T-H. Joubert
Carl and Emily Fuchs Institute for Microelectronics
(CEFIM), University of Pretoria,
Pretoria, South Africa

Abstract*—The work presented details the development of a low-cost potentiostat, with the aim of creating an ink-jet printed hybrid paper-based low-cost sensing system for rapid water quality monitoring. Potentiostats exhibit high sensitivities and can be used for a variety of applications. In this application, they use electrochemical techniques to detect heavy metals via stripping analysis. The potentiostat front-end, consisting of an LMP91000 sensing chip, was designed and manufactured on a printed circuit board (PCB) and compared to a laboratory-based potentiostat using cyclic voltammetry performed using an 80 µl sample of 5 mM ferri-ferrocyanide dropped onto a commercial screen-printed electrode. The results obtained from the PCB potentiostat are comparable to those obtained using the development board and the laboratory-based potentiostat. The results highlight the functionality of a low-cost point-of-need potentiostat that can be used for environmental monitoring as well as the feasibility of transferring the design to a paper substrate.

Keywords— potentiostat, point-of-need, cyclic voltammetry, LMP91000, low-cost

I. INTRODUCTION

The focus of this paper is on the development of a low-cost potentiostat with the aim of creating an ink-jet printed hybrid paper-based low-cost sensing system. This would aid the development of new technologies in the fields of wearables, healthcare, environmental monitoring, packaging and energy provision and storage [1-3]. The first application would be for rapid water quality monitoring.

South Africa faces various challenges regarding water quality and availability. As an example, heavy metal contamination introduced into water supplies can cause serious health and environmental damage [4, 5]. Wet chemical and spectroscopic methods exist to test for heavy metals, however, these methods are timely and expensive and are therefore not suited for point-of-need testing [6]. A need exists to develop effective, low-cost, user-friendly and portable solutions to address these challenges.

A set of criteria has been established by the World Health Organisation (WHO) to which point-of-need diagnostics should adhere. The ASSURED criteria stand for Affordable, Sensitive, Specific, User-friendly, Rapid and Robust, Equipment free and Deliverable to end-users [5]. The implementation of diagnostic tools using paper-based electronics aligns well with these criteria, as a result of beneficial paper properties such as low cost and disposability [5,6]. Furthermore, printed electronics aids the implementation of hybrid circuitry, where a paper substrate populated with off-the-shelf silicon chips enables rapid prototyping and low-cost manufacturing [6-9].

With advances in heterogeneous integration technology, low-power potentiostats can be implemented on paper and similar low-cost substrates [2, 8]. Off-the-shelf potentiostat front-end chips have become available, allowing the functions of previously expensive, laboratory-based potentiostats to be used for the development of point-of-need devices. By utilising processing platforms such as Raspberry Pi [10] or Arduino [11], the implementation cost of potentiostats decreases by more than a factor of 10, compared to existing laboratory equipment [12, 13]. Therefore, interest in the use of potentiostats for environmental point-of-need applications has grown rapidly over the past few years. Potentiostats have a high sensitivity and can be used for a variety of applications such as gas detection, biosensing, ethanol detection and heavy metal detection [2, 3, 14-19].

Potentiostats use electrochemical techniques to detect heavy metals via stripping analyses. By sweeping a potential, metal ions of interest are reduced at specific reduction potentials which generate a current spike at that potential, indicating which heavy metal contaminant is present in the sample within minutes [20].

A potentiostat front-end was manufactured on a printed circuit board (PCB) and was compared to a potentiostat front-end development board and a laboratory-based potentiostat using cyclic voltammetry, performed using an 80 µl sample of 5 mM ferri-ferrocyanide dropped onto a commercial screen-printed electrode. When compared to the development board and the laboratory-based potentiostat, the results obtained from the PCB potentiostat showed similar contour characteristics. The results from the PCB potentiostat

produced redox and oxidation peak current differences of 2.3 µA and 6.3 µA when compared to the laboratory-based potentiostat. These redox and oxidation peaks are indicators of electron transfer characteristics, indicating that the PCB potentiostat is functioning correctly. This forms part of the development towards a fully hybrid paper-based sensing solution for a low-cost point-of-need water monitoring system.

II. Materials and Methods

A. Materials and manufacturing

The PCB potentiostat front-end comprises a sensing chip (LMP91000, Texas Instruments, USA), with required electronic circuitry designed and manufactured on a PCB and connected to an Arduino Uno (Arduino, USA) which controls and communicates with the front-end. The Arduino Uno transmits the sensor data to a personal computer (PC) where the data is read to a Microsoft Excel (2010) template file.

Using this sensing system, cyclic voltammetry was performed using an 80 µl sample of 5 mM ferri-ferrocyanide ($[Fe(CN)_6]^{3-/4-}$) redox coupled with 0.1 M KCl electrolyte. The sample was dropped onto a commercially available screen printed ceramic electrochemical sensor (DS-C110, Dropsens, Spain). The data was compared to both a development board (LMP91000EVM, Texas Instruments, USA) and a laboratory-based potentiostat (Autolab PGSTAT, Metrohm, Germany). Fig.1 shows a schematic diagram of the experiment.

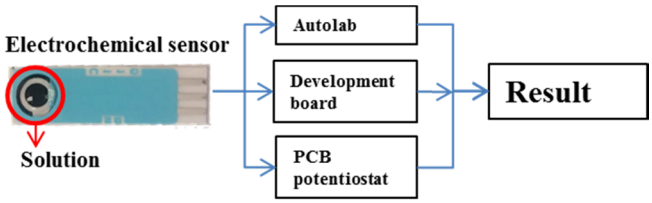

Fig. 1. A schematic diagram of the electrochemical experiment.

B. Experimental procedures

Using a drop sensing approach, the sample was dispensed onto the centre of the three electrode surface as displayed in Fig.1. Cyclic voltammetry was performed three times for each sensing system at a scan rate of 50 mVs^{-1} ranging from -0.6 V to 0.6 V. The cyclic voltammograms were generated using either the PCB potentiostat system, development board or the Autolab. The various sensing systems are shown in Fig. 2.

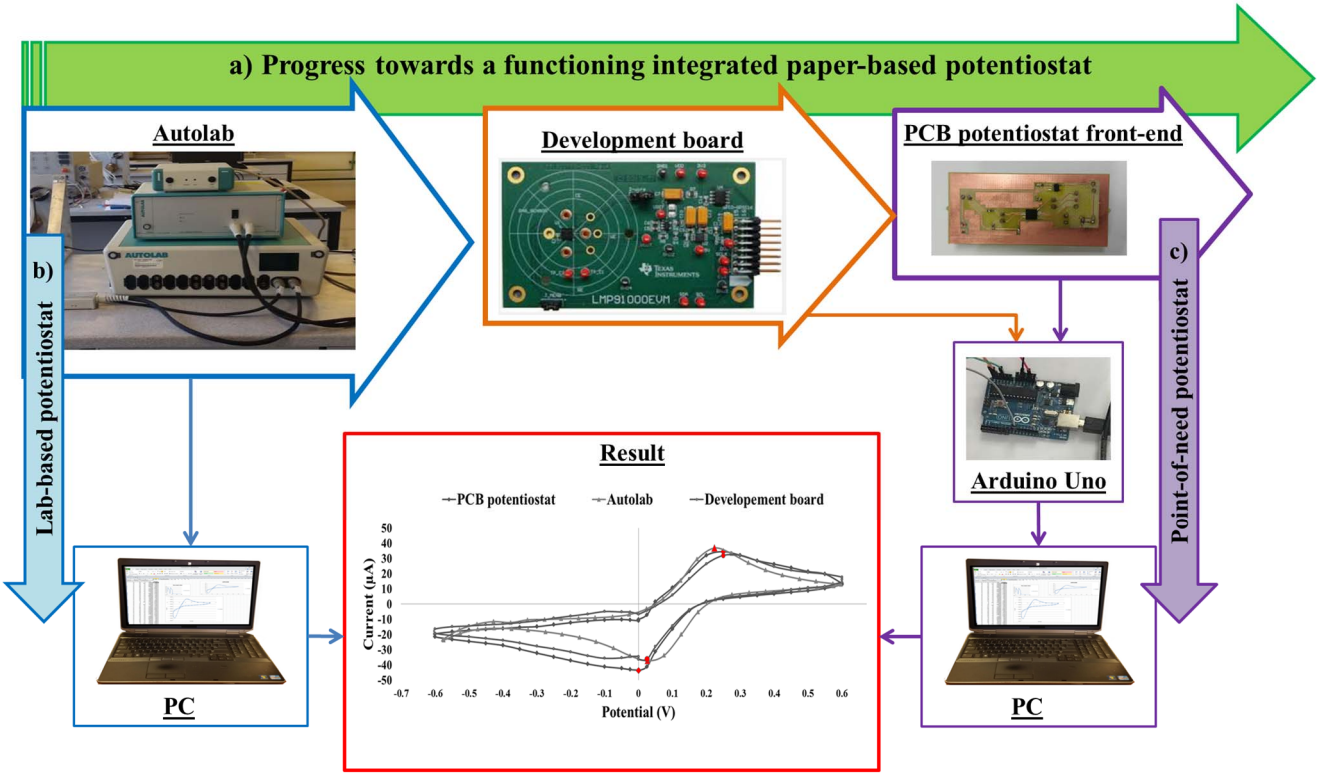

Fig. 2. A development diagram of the point-of-need potentiostat, depicting (a) the development towards a printed paper-based potentiostat, (b) the process followed by the Autolab to generate a result and (c) the process followed by the development board and the PCB potentiostat to produce a result.

C. Design and development of the potentiostat

The registers of the PCB potentiostat front-end were programmed using the Arduino UNO via I2C communication. The registers are controlled by the Arduino and are used for functions such as gain, input waveform generation and mode selection for the electrochemical experiment. The Trans-impedance Control Register (TIACN) is used to program the trans-impedance amplifier gain (RTIA), which was selected as 35 kΩ, and the load impedance (RL), selected as 10 Ω. The reference control register (REFCN) determines the voltage source selection, internal zero selection, positive or negative bias as well as the level of bias introduced to the system. By utilising an external reference source a larger voltage sweeping range can be implemented, however for this application the internal reference voltage of 2.5 V was selected, therefore no external supply was needed. The internal zero can be set at 20 %, 50 %, 60 % or can be bypassed. For this application, the internal zero was set at 50 % because a reversible electrochemical reaction was expected (redox and oxidation current peaks have similar absolute heights) [21]. The input voltage can be swept from 0 % to 24 % by changing the percentage reference voltage used, and by changing the bias sign (negative or positive) to generate a sweeping range from -0.6 V (-24 %) to 0.6 V (24 %). The reference voltage defines the voltage range over which the sweep will occur and the internal zero defines around what % voltage the bias will swing. Therefore, the input signal has a voltage range of 1.2 V using 48 steps, generating a scan rate of 50 mVs^{-1}. The output current was calculated using (1) [13].

$$I_{out} = (V_{out} - V_{ref})/ R_{TIA} \quad (1)$$

The node control register (MODECN) was used to define the system as a three electrode system. For cyclic voltammetry, the input potential will be swept from negative to positive and positive to negative. The lab-based approach using the Metrohm Autolab is compared to the development board and the PCB potentiostat in Fig. 2. Fig. 2 (b) shows the process the Autolab follows to generate a result and Fig. 2 (c) depicts the process diagram of the development board and the point-of-need potentiostat, starting with LMP91000 potentiostat front-end connected to an Arduino UNO. The Arduino is used for communication between the potentiostat front-end and the PC which is used for data analyses. A program called Gobetwino [22] is used to prompt the Arduino to start the experiment as well as to save and plot the data in a personalised Microsoft® Excel template file where the data is automatically graphed.

The development towards the printed potentiostat shown in Fig.2 (a) includes the transition phases from the Autolab up to the PCB potentiostat. This approach enables parallel product development, where for example, paper-based circuitry and back-end development can occur independently and can be integrated at a later stage.

The PCB potentiostat front-end design is shown in Fig. 3 and can be directly transferred to a paper-based design. The development board has a built-in ADC and EEPROM circuit. Because the Arduino Uno can perform similar functions, the PCB potentiostat front-end only consists of the LMP91000 chip, voltage reference and relevant passive components as seen in Fig. 3 (a). Furthermore, if an external reference voltage provided by the Arduino UNO is used, the voltage reference chip (MP4120AIM5-2.5) can also be excluded which simplifies the circuit further. The PCB layout design in Fig. 3 (b) was designed in Altium [24] and can be exported as a DXF to enable the manufacture of an ink-jet printed paper-based circuit, similar to previous work [25]. The large ground plane serves as a current return path for all grounded components, makes design easier, ensures all the components are at the same reference potential and reduces noise and ground-loop interferences.

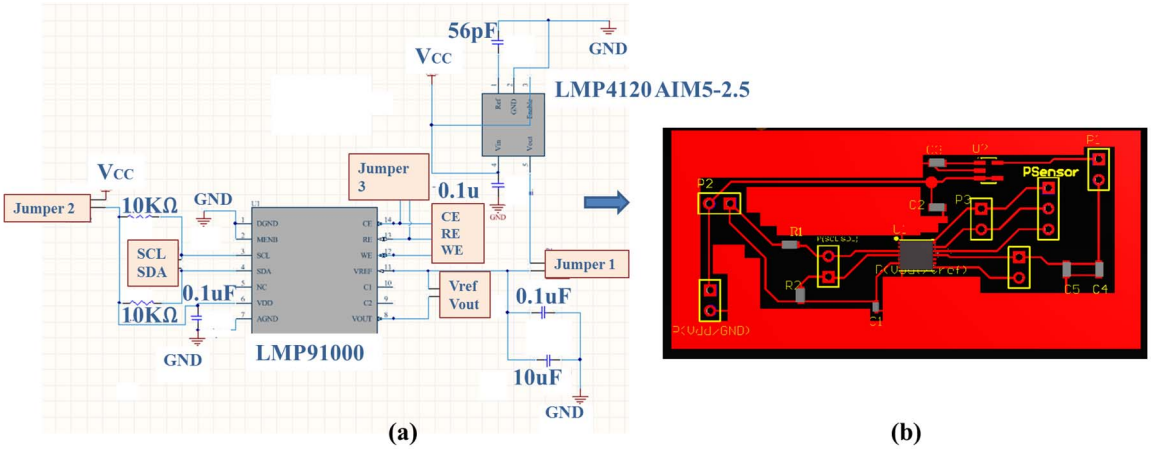

Fig. 3. Point-of-need potentiostat (a) schematic diagram and (b) PCB layout design[23].

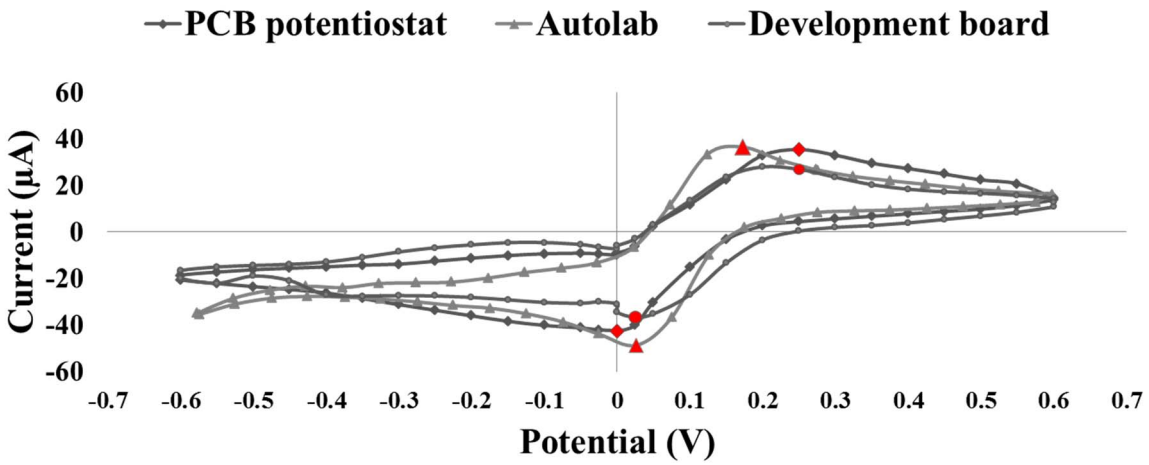

Fig. 4. Comparison of the cyclic voltammograms generated from the average of three experiments using either the Autolab, development board or the PCB potentiostat. The red markers indicate the peak redox and oxidation currents of each sensing system respectively.

III. Results and Discussion

The electrochemical performance of the development board and PCB potentiostat was validated and compared to the Autolab in Fig. 4 by performing three sets of cyclic voltammetry tests for each sensing system, on three Dropsens electrodes in a 0.1 M KCL solution containing 5 mM $[Fe(CN)_6]^{3-/4-}$ at a 50 mVs^{-1} scan rate.

In Fig. 4 the development board and PCB potentiostat produce more signal noise than produced by the Autolab. The vertical jump in data that occurs when the potential is zero for the development board and PCB front-end is due to noise generated by the change in the LMP91000 registers (positive to negative or negative to positive). The standard deviation and averages of the three sets of experiments using each sensing system are shown in Table I.

TABLE I.
THE STANDARD DEVIATION (SD) AND AVERAGE (AVG) OBTAINED FROM THREE REPEATS OF EACH EXPERIMENT USING THE AUTOLAB, DEVELOPMENT BOARD AND PCB POTENTIOSTAT.

	Autolab		**Development board**		**PCB potentiostat**	
	AVG	**SD**	**AVG**	**SD**	**AVG**	**SD**
Redox current peak (µA)	35.2	2.4	31.7	1.3	37.5	0.7
Oxidation current peak (µA)	-34.7	3.7	-40.4	5.1	-41.0	1.3

The absolute values of redox and oxidation currents of the Autolab are similar which indicate that the electrochemical process of the Autolab was closer to a reversible system than that of the other two systems [21]. The cyclic voltammetry curves of the redox and oxidation currents of the three systems are similar, indicating that even though the development board and the PCB potentiostat may require further optimisation, each of the systems shows repeatability across the three experiments performed.

The results expressed in Table II show the difference between the Autolab and the development board or the PCB potentiostat, as compared to a similar set-up reported in literature [13]. The table shows the percentage difference between the peak as measured by the Autolab and the peak measured by the described system, illustrating that the developed PCB potentiostat compares well to large-scale laboratory equipment and similar reported results.

TABLE II.
A COMPARISON BETWEEN THE REPORTED SYSTEM AND A SIMILAR SYSTEM IN LITERATURE.

	Development board used in literature [13]	**Development board**	**PCB potentiostat**
Redox current peak difference (%)	8.3	10.2	6.4
Oxidation current peak difference (%)	15.4	16.5	18.1

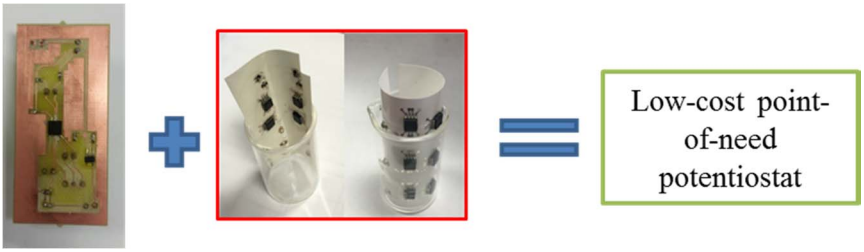

Fig. 5. The transition from the PCB potentiostat front-end to a functioning paper-based potentiostat [7].

Next steps will focus on the optimisation of the PCB potentiostat to test for heavy metals in a solution. Further development includes activities such as the integration of the PCB front-end onto a paper substrate as illustrated in Fig. 5. In Fig. 5 an example of repeatable and flexible interconnects between off-the-shelf components and a paper-based substrate using ink-jet printing is used to illustrate the integration process being followed to produce a hybrid ink-jet printed paper-based potentiostat.

IV. Conclusion

The development towards a point-of-need, low-cost potentiostat has been presented and will assist in a variety of applications such as biosensing, gas, ethanol and heavy metal detection. The developed PCB potentiostat delivers comparable results to those produced by a lab-based potentiostat. Furthermore, the design used for the PCB potentiostat front-end can directly be used to manufacture an ink-jet printed circuit design. The next steps include creating a hybrid paper-based low-cost potentiostat for environmental diagnostics. This will provide a low cost, point-of-need solution that can be rapidly prototyped.

Acknowledgements

The authors gratefully acknowledge the Council for Scientific and Industrial Research (CSIR) in Pretoria for funding the project and funding from the NRF used by the University of Pretoria to fund this conference.

References

[1] IDTechEx Raghu Das, Printed, flexible and hybrid electronics: hot trends and market outlook, 2017.

[2] A.P.F. Turner, "The Paper Potentiostat," in *4th International Conference on Biosensing Technology*, Lisbon, Portugal, 2015.

[3] J. Kim, I. Jeerapan, S. Imani, T. Cho, A. Bandodkar, S. Cinti, P. Mercier and J. Wang, "Noninvasive alcohol monitoring using a wearable tattoo-based iontophoretic-biosensing system," *ACS Sensors*, p. 1011−1019, July 2016.

[4] P.B. Tchounwou , C.G. Yedjou, A.K. Patlolla and D.J. Sutton, "Heavy Metals Toxicity and the Environment," National Institute of Health Public access, Aug. 2012.

[5] D. Mabey, R.W. Peeling, A. Ustianowski and M. Perkins, "Diagnostics for the developing world," Nat. Rev., vol. 2, no. 3, pp. 231-240, 2004.

[6] S. Smith, P. Bezuidenhout, M. Mbanjwa, H. Zheng, M. Conning, N. Palaniyandy, K. Ozoemena and K. Land, "Development of paper-based electrochemical sensors for water quality monitoring," *Fourth Conference on Sensors, MEMS and Electro-Optic Systems, International Society for Optics and Photonics*, February 2017.

[7] P.H. Bezuidenhout K.J. Land and T-H. Joubert, "Integrating integrated circuit chips on paper substrates using ink-jet printed electronics," in *17th Annual International Conference of the Rapid product development association of South-Africa*, VUT Southern Gauteng Science and Technology Park, 2016.

[8] P. Bezuidenhout, K. Land and T-H. Joubert, "A low-power CMOS operational amplifier IC for a heterogeneous paper-based potentiostat," in *Fourth Conference on Sensors, MEMS and Electro-Optic Systems. International Society for Optics and Photonics*, 2017, pp. 100360P-100360P.

[9] J. Miettinen, V. Pekkanen, K. Kaija, P. Mansikkamaki, J. Mantysalo, M. Mantysalo, J. Niittynen, J. Pekkanen, T. Saviauk and Ri. Ronkka, "Inkjet printed System-in-Package design and manufacturing," *Microelectronics Journal*, vol. 39, pp. 1740–1750, April 2008.

[10] Raspberry Pi. (2017, April) Raspberry Pi. [Online]. https://www.raspberrypi.org/

[11] Arduino. (2017, April) Arduino. [Online]. https://www.arduino.cc/

[12] C. Harnett, "Open source hardware for instrumentation and measurement," *IEEE Instrumentation & Measurement Magazine*, vol. 11, pp. 34 – 38, 2011.

[13] N. Norena, A. Kaushik, S. Bhansali and A. Cruz, "A low-cost miniaturised potentiostat for point-of-care diagnosis," *Biosensors and Bioelectronics*, vol. 62, pp. 249-254, 2014.

[14] C-C Chen and G-N Sung, W-C Chen, C-T Kuo, J-J Chue, C-M Wu, C-M Huang, "A wireless and batteryless intelligent carbon monoxide sensor," *Sensors*, vol. 16, pp. 1568-1579, September 2016.

[15] P. Mostafalu, W. Lenk, M.R. Dokmeci, B. Ziaie, A. Khademhosseini and S.R. Sonkusale, "Wireless flexible smart bandage for continuous monitoring of wound oxygenation," *IEEE Transactions on biomedical circuits and systems*, vol. 9, no. 5, pp. 670-677, October 2015.

[16] F. Basilotta, S. Riario, F. Stradolini, I. Taurino, D. Demarchi, G. De Micheli and S. Carrara, "Wireless monitoring in intensive care units by a 3D-Printed system with embedded electronic," *IEEE*, 2015.

[17] G. Jasinski, A. Strzelczyk and P. Koscinski, "Low cost electrochemical sensor module for measurement of gas concentration," in *39th International Microelectronics and Packaging IMAPS Poland 2015 Conference*, 2015.

[18] M. B. Marinov, I. Topalov, E. Gieva and G. Nikolov, "Air quality monitoring in urban environments," in *39th International Spring Seminar on Electronics Technology (ISSE)*, 2016.

[19] A. Kaushik, A. Yndart, R. Dev Jayant, V. Sagar, V. Atluri, S. Bhansali and M. Nair, "Electrochemical sensing method for point-of-care cortisol detection in human immunodeficiency virus-infected patients," *International Journal of Nanomedicine*, vol. 10, pp. 677–685, 2015.

[20] Z. Zou, A. Jang, E. McKnight, P.-M. Wu, J. Do, P. Bishop and C. Ahn, "Environmentally friendly disposable sensors with microfabricated on-chip planar bismuth electrode for in situ heavy metal ions measurement," *Sensors and Actuators B: Chemical*, vol. 134, pp. 18–24, Apr. 2008.

[21] Princeton applied research, A Review of Techniques for Electrochemical Analysis, Application Note E-4.

[22] MikMo. (2017, April) Gobetwino. [Online]. http://mikmo.dk/gobetwinodownload.html

[23] Texas Instruments, LMP91000EVM User's Guide, 2012.

[24] Altium. (2017, April) Altium. [Online]. http://www.altium.com/

[25] P. Bezuidenhout and J. Schoeman, T-H. Joubert, "The Design and Manufacturing Considerations of a Paper-Based E. coli Biosensor," in *International Conference on Competitive Manufacturing*, Stellenbosch, 2016.